

Quasi-periodic resonances and the Landau-Hopf scenario

© A.P. Kuznetsov, Yu.V. Sedova

Saratov Branch, Kotelnikov Institute of Radio Engineering and Electronics, Russian Academy of Sciences,
410019 Saratov, Russia
e-mail: sedovayv@yandex.ru

Received March 25, 2025

Revised June 4, 2025

Accepted June 4, 2025

The effect of resonances on a cascade of quasi-periodic bifurcations, the sequence of which occur in accordance with the Landau-Hopf scenario, is examined using an ensemble of discrete van der Pol - Duffing oscillators. With small frequency detunings of the oscillators, tongues of quasi-periodic modes emerge, analogous to Arnold tongues, and in the region of the highest frequency oscillations. With a large frequency detuning, the general structure of regimes transformation in accordance with Landau-Hopf scenario remains, but the quasi-periodic Hopf bifurcation in the cascade can be replaced by a saddle-node bifurcation of torus. Narrow resonance regions based on tori of different dimensions are also observed. At high values of the Duffing oscillator-like nonlinear parameter, resonances can destroy high-dimensional tori in the Landau-Hopf cascade.

Keywords: quasi-periodicity, resonance, Landau-Hopf scenario, Lyapunov exponents, bifurcations.

DOI: 10.61011/TP.2025.11.62227.46-25

Introduction

Quasi-periodic oscillations are quite common in nature and technology. They can be characterized by different, sometimes quite a large number of incommensurable frequencies. Such examples can be found in radiophysics and electronics [1–9], in the theory of Josephson contacts [10–12], mechanics and hydrodynamics [13–18], many examples are known in astrophysics [19,20], as well as in other areas. Quasi-periodic oscillations with different numbers of incommensurable frequencies are also studied using examples of model discrete systems (maps), in particular, in Ref. [21–25].

At one time, Landau and Hopf associated the scenario of the emergence of complex (chaotic) dynamics with quasi-periodic oscillations [26,27]. The scenario assumes a gradual increase in the number of incommensurable frequencies due to the coupling of new oscillatory modes. This process occurs through a cascade of quasi-periodic Hopf bifurcations, as a result of which invariant tori of ever higher dimension are born in the phase space. A general discussion about such a scenario is discussed in many works, for example, in Ref. [14–17,28–30].

Formally, the Landau-Hopf scenario assumes an infinite number of quasi-periodic bifurcations. However, more realistic situations where the number of bifurcations is relatively high, but of course, are of considerable interest from the point of view of the mechanisms of occurrence of complex oscillations. The Landau-Hopf cascade can be disrupted by destroying the torus to create chaos. As you know, Ruel and Takens drew attention to this point [31], which caused a subsequent discussion and an active discussion. At the same time, Afraimovich and Shilnikov found that a two-dimensional two-frequency torus

can collapse with the formation of chaos [32]. However, there are now known examples of stable tori of sufficiently high dimension corresponding to four-, five-, and even six-frequency oscillations [4–6,8–10,18,21,22,24,25].

The cascade of quasi-periodic bifurcations can also be limited by a finite number of oscillation modes of the system itself. For example, an ensemble of five self-oscillating van der Pol oscillators is considered in Ref. [33] that demonstrates five steps of the Landau-Hopf scenario. Let us emphasize here the universal character of the van der Pol system, which describes both a radiophysical generator and systems of a wide variety of nature, see Ref. [34] and the review in Ref. [35]. Interestingly, the interaction of the [33] system with an additional chaotic subsystem does not decrease, but increases the number of quasi-periodic bifurcations and the possible dimension of the torus [36].

From the point of view of oscillation theory, it seems that another mechanism for breaking the cascade of Landau-Hopf bifurcations may be the occurrence of synchronization and corresponding resonances on high-dimensional tori. It is this aspect that we will consider in this paper.

As is known, in the simplest case of two-frequency quasi-periodicity, resonant limit cycles can occur on the surface of the corresponding attractor in the form of an invariant torus. This transition is provided by the saddle-node bifurcation of the limit cycles. In this case, a structure of Arnold tongues embedded in the region of quasiperiodicity arises on the parameter plane [34,37,38]. Over time, it became known that synchronization of multi-frequency quasi-periodic oscillations is also possible, when a torus of a smaller dimension is born on the surface of a high-dimensional torus. Such a transition occurs through the bifurcation of the tori [39,40] caused by the collision of the stable and saddle tori. Early examples

for radiophysical generators can be found, for example, in Ref. [4–6]. At the same time, on the parameter plane, in a situation of synchronization of multi-frequency oscillations, a pattern may appear similar to the Arnold tongue system, but in the form of tongues of quasi-periodic modes. It has been observed in model maps in Ref. [25,41], coupled radiophysical generators [8,9,42], predator-prey system [43] and other examples.

In this paper, we will examine the relationship between the Landau-Hopf bifurcation diagram and potential resonances.

1. Studied system. Case of absence of resonances

A system of five dissipatively coupled non-identical van der Pol oscillators was proposed in Ref. [33,36] in the context of the Landau-Hopf scenario. Five steps of the Landau-Hopf scenario are consistently observed in such a system, when the coupling value decreases (analogous to the Reynolds number). As is known, for two coupled Van der Pol oscillators, high resonances, unlike the main one, are poorly expressed, especially in the case of small values of the excitation parameters [44,45]. Therefore, firstly, we use increased values of these parameters compared to Ref. [33,36]. Secondly, we will supplement this model with cubic nonlinearity of the Duffing oscillator type. Physically, this nonlinearity is responsible for the non-isochronous nature of small oscillations [34]. In the case of two oscillators, this leads to a much more pronounced system of resonant tongues of different orders [46].

We also use a discrete version of the system to simplify the analysis. It is obtained by replacing the time derivatives in the original equations with finite differences. A similar technique was proposed in early papers on nonlinear physics [47–49]. It is now widely used in a wide variety of fields: radiophysics, population dynamics, neurodynamics, theory of gene networks, as well as in describing basic models of oscillation theory and nonlinear dynamics (a number of specific examples can be found in the overview section [25]). Moreover, if we use a small value of the discretization parameter, then the arrangement of regions in the parameter space will be very close to the prototype system with continuous time. At the same time, analyzing a discrete system is much simpler.

Taking into account these observations, the system under study has the form

$$\begin{aligned} x_{i,n+1} &= x_{i,n} + \varepsilon y_{i,n+1}, \\ y_{i,n+1} &= y_{i,n} + \varepsilon(\lambda_i - x_{i,n}^2)y_{i,n} - \varepsilon(1 + \Delta_{i-1})x_{i,n} \\ &\quad - \varepsilon\beta x_{i,n}^3 - \varepsilon \frac{\mu}{4} \sum_{j=1}^5 (y_{i,n} - y_{j,n}) \end{aligned} \quad (1)$$

Here $x_{i,n}$, $y_{i,n}$ are variables (coordinate and velocity) of the i th oscillator, λ_i is its excitation parameter, β is the

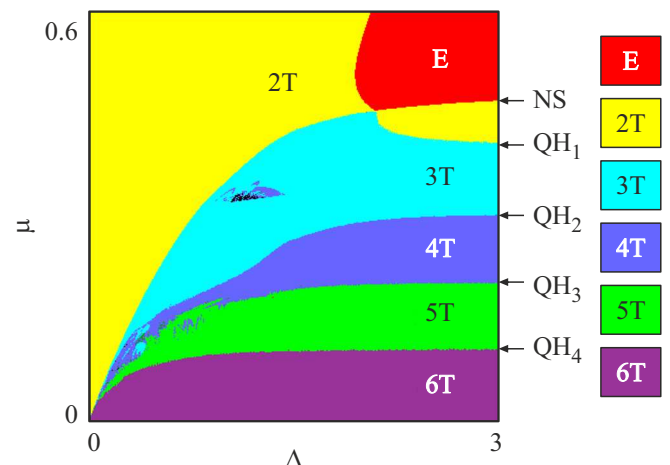


Figure 1. Chart of Lyapunov exponents of an ensemble of five discrete van de Pol oscillators (1) for $\lambda_1 = 0.1$, $\lambda_2 = 0.2$, $\lambda_3 = 0.3$, $\lambda_4 = 0.4$, $\lambda_5 = 0.5$, $\varepsilon = 0.1$. Cubic nonlinearity parameter $\beta = 0$.

parameter of additional nonlinearity according to the type of Duffing oscillator, μ is the magnitude of the dissipative coupling. $\Delta_{i-1} = \Delta(i-1)/4$ are frequency detunings of the oscillators relative to the first one, the frequency of which is taken as one. In this case, the mutual detunings of the oscillators are controlled by a single parameter Δ . In addition, n is the iteration number, ε is the discretization parameter.

Following Ref. [33,36], we first put $\lambda_1 = 0.1$, $\lambda_2 = 0.2$, $\lambda_3 = 0.3$, $\lambda_4 = 0.4$, $\lambda_5 = 0.5$. Here and further we will use the small value $\varepsilon = 0.1$. For further discussion, we will first present the case of the absence of additional nonlinearity $\beta = 0$. Fig. 1 shows the corresponding chart of Lyapunov exponents on the frequency detuning coupling value plane (Δ , μ). On this chart, areas with different dynamics are indicated in different colors in accordance with the signature of the spectrum of Lyapunov exponents Λ_n , as indicated in the table. There are six significant exponents in this table, the rest are always negative. The interpretation of the color palette is shown to the right of the picture.

When coupling value μ decreases along the right edge of the chart, with a frequency disorder of $\Delta = 3$, an equilibrium state E is first observed. Then, as a result of the Neimark-Sacker bifurcation NS, a stable invariant curve is separated from it, which corresponds to the birth of the two-frequency 2T regime. Then, a two-dimensional torus separates from this curve as a result of quasi-periodic Hopf bifurcation and a three-frequency 3T regime is born at point QH₁. Next, a cascade of quasi-periodic Hopf bifurcations QH_{2,3,4} occurs, with the gradual birth of four-, five-, and six-frequency regimes 4T, 5T, and 6T. (As we noted, due to smallness, ε the configuration of the regions and the nature of the bifurcations are similar to the case of the flow system [33], with the exception of an increase in the number of frequencies occurring by one, which is typical for discrete systems.)

Types of regimes and the Lyapunov exponents spectrum for map

Designation	Regime type	Type of attractor in the map	Spectrum of Lyapunov exponents
E	Equilibrium	Fixed point	$\Lambda_{1,2,3,4,5,6} < 0$
2T	Two-frequency quasi-periodic	Invariant curve	$\Lambda_1 = 0, \Lambda_{2,3,4,5,6} < 0$
3T	Three-frequency quasi-periodic	Two-dimensional torus	$\Lambda_{1,2} = 0, \Lambda_{3,4,5,6} < 0$
4T	Four-frequency quasi-periodic	Three-dimensional torus	$\Lambda_{1,2,3} = 0, \Lambda_{4,5,6} < 0$
5T	Five-frequency quasi-periodic	Four-dimensional torus	$\Lambda_{1,2,3,4} = 0, \Lambda_{5,6} < 0$
6T	Six-frequency quasi-periodic	Five-dimensional torus	$\Lambda_{1,2,3,4,5} = 0, \Lambda_6 < 0$
C	Chaos	Chaotic attractor	$\Lambda_1 > 0, \Lambda_{2,3,4,5,6} < 0$
H	Hyperchaos	Hyperchaotic attractor	$\Lambda_{1,2} > 0, \Lambda_{3,4,5,6} < 0$

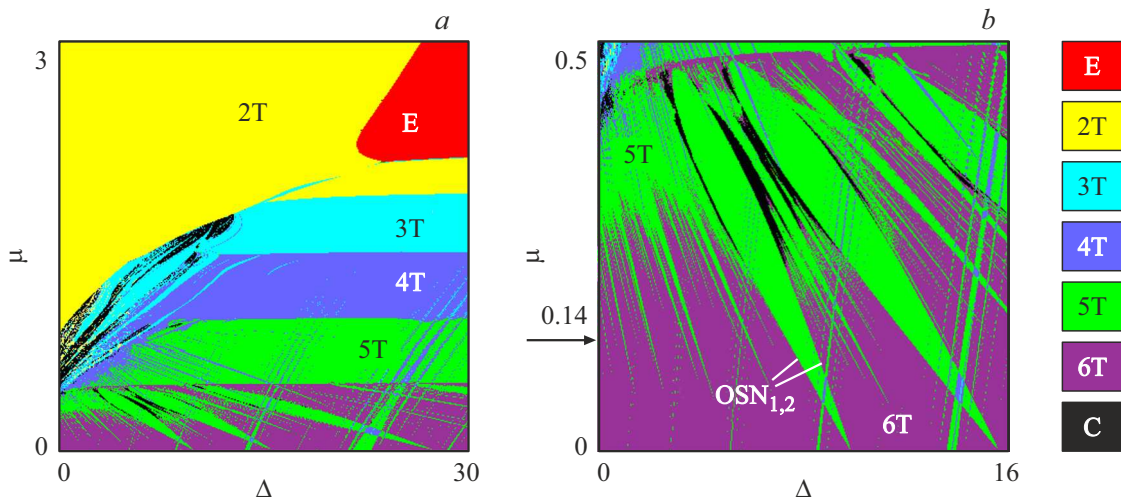


Figure 2. Chart of Lyapunov exponents of an ensemble of five discrete Van der Pol-Duffing oscillators for $\beta = 1$ (a) and its enlarged fragment (b). The arrow marks the value $\mu = 0.14$ corresponding to the graphs in Fig. 3. Parameter values: $\lambda_1 = 0.5, \lambda_2 = 1, \lambda_3 = 1.5, \lambda_4 = 2, \lambda_5 = 2.5, \varepsilon = 0.1$.

As can be seen from Fig. 1, there are no resonant regimes (except for the main resonance $\Delta = 0$) in the case of small parameters of excitation λ and in the absence of additional nonlinearity. At the same time, five steps of the Landau-Hopf cascade are observed with a sufficiently large frequency detuning Δ , with a decrease in the magnitude of the dissipative coupling μ .

2. Case of quasi-periodic resonances

Now let us increase the control parameters so that $\lambda_1 = 0.5, \lambda_2 = 1, \lambda_3 = 1.5, \lambda_4 = 2, \lambda_5 = 2.5$ and select the value the additional nonlinearity parameter $\beta = 1$ by analogy with Ref. [46]. The corresponding Lyapunov chart is shown in Fig. 2, a. Now there are characteristic quasi-periodic resonances. This is especially noticeable for the six-frequency region. The corresponding enlarged fragment of the chart is shown in Fig. 2, b. It is possible to

see the emergence of tongues similar to the traditional Arnold tongues, but based on high-dimensional 6T tori and corresponding to the five-frequency 5T regimes. The largest tongues have cusps on the frequency detuning axis Δ . It should be noted that the resonances are more pronounced the lower the frequency detuning Δ of the oscillators.

Resonances are also present in the range of five-frequency 5T and four-frequency 4T regimes, but they are less pronounced. They are practically absent in the three- and two-frequency regions of 3T and 2T. Thus, resonances primarily occur in the highest frequency regions.

Another feature of the picture in Fig. 2, b is the appearance of chaos C in the area of overlapping five-frequency tongues. There was no chaos in Fig. 1. It can be also seen in the range of $0 < \Delta < 10$ in Fig. 2, a that chaos is now possible in the area of localization of three-frequency tongues 3T — they are immersed in the area of chaos. However, in general, the areas of chaos are small in size.

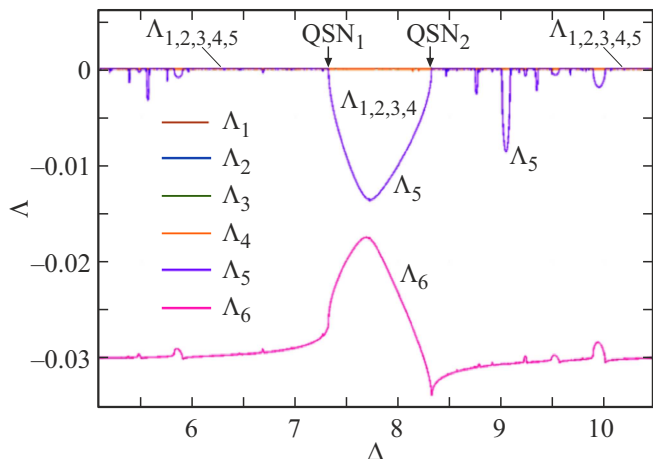


Figure 3. Graphs of Lyapunov exponents along the line $\mu = 0.14$. Values of parameters: $\lambda_1 = 0.5$, $\lambda_2 = 1$, $\lambda_3 = 1.5$, $\lambda_4 = 2$, $\lambda_5 = 2.5$, $\varepsilon = 0.1$ and $\beta = 1$. $QSN_{1,2}$ — points of saddle-node bifurcations of the torus.

The resonant nature of quasi-periodic tongues is illustrated in Fig. 3. It shows graphs of Lyapunov exponents along a segment of the horizontal line $\mu = 0.14$ in the range of $5.1 < \Delta < 10.5$, intersecting one of the largest tongues and several small ones. This relationship value is indicated by an arrow in Fig. 2, *b*. A six-frequency 6T mode with zero values $\Lambda_{1,2,3,4,5} = 0$ is observed on the graphs outside the resonant regions. The parameters $\Lambda_{1,2,3,4} = 0$ are zero inside the resonant regions, and the fifth Λ_5 is negative, so the five-frequency 5T regime is implemented. At the same time, the sixth parameter Λ_6 is also negative, and nowhere near the boundaries of the tongue does it coincide with Λ_5 . According to Ref. [39,40], this is a sign of a quasi-periodic saddle-node bifurcation of the torus. Such bifurcations for the largest tongue are marked with arrows in Fig. 3 and are indicated by $QSN_{1,2}$. Also, the corresponding boundaries of the tongue are marked on the parameter plane in Fig. 2, *b*. Thus, we are indeed observing resonant charts. Their characteristic feature are „dips“ of the corresponding parameter (in this case Λ_5) in the graphs in the negative area.

The width of the resonant tongues noticeably decreases on the chart, Fig. 2, *a* with large frequency detunings of the order of $\Delta = 30$, and the alternation of regions characteristic of the Landau-Hopf cascade occurs again with a variation of the coupling μ . However, the required value of the frequency detuning Δ increases tenfold compared to Fig. 1. Thus, a large mutual frequency detuning of the oscillators is required for the effect of resonances to be not very significant. But even in this case, there are some peculiarities. Let's discuss the observed structure and these features in more detail.

To do this, let's turn to the graphs of Lyapunov exponents depending on the magnitude of the coupling μ at $\Delta = 30$ (right edge of the chart in Fig. 2, *a*) in the range of $0 < \mu < 2$ shown in Fig. 4. It is possible to see the presence

of characteristic areas dominated by NT modes with a corresponding number of zero values and incommensurable frequencies. For ease of perception, their areas are indicated in the figure by symbols in circles. Let's discuss the observed bifurcations.

The exponent is $\Lambda_1 = 0$ in the right part of the figure, and the rest exponents are negative. In accordance with the table, a two-frequency 2T regime with an attractor in the form of an invariant curve is observed. When approaching the point QH_1 , the second and third exponents are equal to each other: $\Lambda_2 = \Lambda_3$. They are negative and increase with decreasing coupling. Immediately at the point QH_1 , both exponents become zero, and then the exponent Λ_2 remains zero, so now $\Lambda_{1,2} = 0$, and the exponent Λ_3 goes into the negative region. In accordance with Ref. [39], the condition $\Lambda_2 = \Lambda_3$ corresponds to the quasi-periodic Hopf bifurcation QH_1 , when a two-dimensional torus corresponding to the three-frequency 3T regime is gently generated from an invariant curve.

Similarly, when approaching the point QH_2 , the condition $\Lambda_3 = \Lambda_4 < 0$ is fulfilled, so that a quasi-periodic Hopf bifurcation of the birth of a three-dimensional torus is observed, corresponding to the transition from the three-frequency regime 3T to the four-frequency regime 4T. At the same time, resonances in the region of two- and three-frequency regimes and near the point QH_2 are not observed. Therefore, the first stages of the Landau-Hopf cascade are being implemented in this area.

However, then some peculiarities arise. They are illustrated by an enlarged fragment of the Figure in the vicinity of the transition point from the 4T regime to the five-frequency 5T regime, shown in Fig. 5, *a*.

When approaching this point on the right, the exponents $\Lambda_{1,2,3} = 0$, and the exponents Λ_4 and Λ_5 coincide. This is typical for a quasi-periodic Hopf bifurcation of the corresponding order. However, in the immediate vicinity

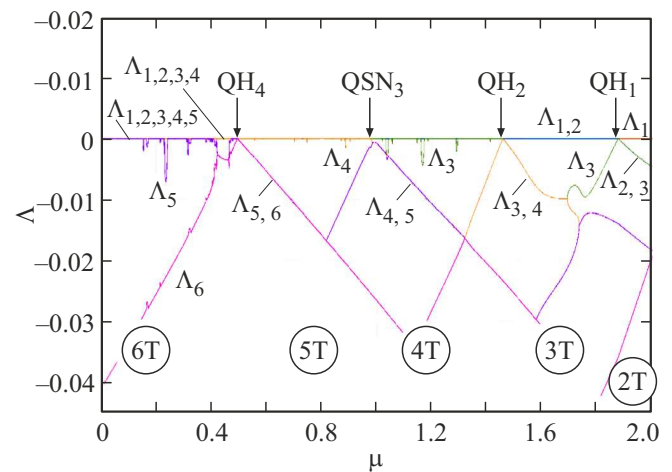


Figure 4. Graphs of Lyapunov exponents depending on the magnitude of μ coupling along the line $\Delta = 30$ for $\beta = 1$. The values of the other parameters: $\lambda_1 = 0.5$, $\lambda_2 = 1$, $\lambda_3 = 1.5$, $\lambda_4 = 2$, $\lambda_5 = 2.5$, $\varepsilon = 0.1$.

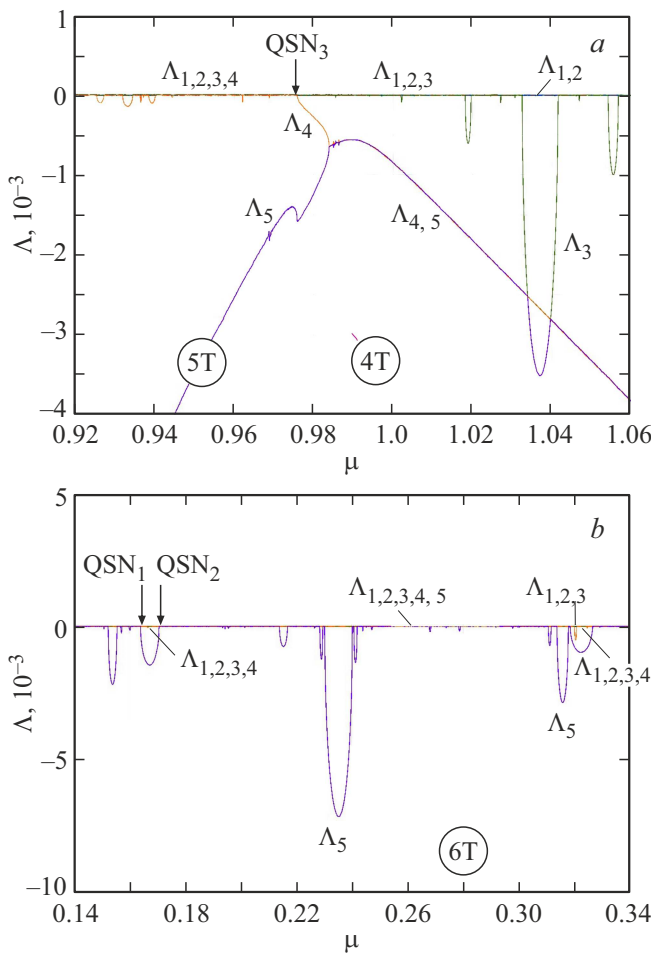


Figure 5. Enlarged fragments of Fig. 4: *a* — the neighborhood of the transition point from four-frequency to five-frequency regime; *b* — the area of six-frequency regimes.

of the transition point, the graphs of exponents Λ_4 and Λ_5 diverge. At the same time, the exponent Λ_5 goes into the negative region, and the exponent Λ_4 increases, becoming zero at the point QSN_3 . In accordance with Ref. [39,40], this behavior corresponds to the saddle-node bifurcation of tori. Thus, one of the quasi-periodic Hopf bifurcations in the Landau-Hopf cascade can be replaced by a saddle-node bifurcation. However, in the vicinity of the point of such a bifurcation, the behavior characteristic of a quasi-periodic Hopf bifurcation persists. So, on a large scale in Fig. 4 near the point QSN_3 , the behavior of the exponents is visually characteristic of the quasi-periodic Hopf bifurcation. This combined behavior can be explained by the fact that the Hopf bifurcation point fell into the vicinity of a certain resonance.

We also note that narrow resonance windows based on tori of different dimensions are now observed. Characteristic “dips” of the third exponent Λ_3 , corresponding to three-frequency resonances based on a four-frequency 4T torus can be seen on the magnified Fig. 5, *a*. The largest of them is marked with the symbol $\Lambda_{1,2}$, indicating the zero value

of these two exponents. There are several less pronounced resonances of this type. There are many very small four-frequency resonances to the left of the point QSN_3 .

Let's return to Fig. 4. A quasi-periodic Hopf bifurcation QH_4 occurs again with a further decrease in coupling in accordance with the condition $\Lambda_5 = \Lambda_6$ producing a six-frequency 6T mode. It can be noted that very close to the point QH_4 , a relatively wide five-frequency resonance is observed to the left of it, marked in Fig. 4 with an arrow and signed with the symbol $\Lambda_{1,2,3,4}$. Generally, resonances in the six-frequency region are most pronounced. They are illustrated by an enlarged fragment of graphs in Fig. 5, *b*. It is possible to see the area of six-frequency regimes with $\Lambda_{1,2,3,4,5} = 0$, which has built-in five-frequency resonances with $\Lambda_{1,2,3,4} = 0$. Their boundaries are also the points of saddle-node bifurcations of the QSN tori. An interesting feature can be seen for the resonant window located on the right side of Fig. 5, *b*. There is a (albeit very narrow) area with $\Lambda_{1,2,3} = 0$ inside it. Thus, a secondary resonance with the appearance of a four-frequency torus is possible on the surface of a resonant five-frequency torus. Characteristic small islands lying at the intersection of five-frequency tongues correspond to them on the charts in Fig. 2.

Thus, quasi-periodic resonances based on high-frequency tori can occur with a certain selection of parameters in a system with the Landau-Hopf scenario. However, the resonances are narrow with a sufficiently large frequency detuning of the oscillators and generally do not destroy the Landau-Hopf scenario.

3. The case of large values of the nonlinearity parameter according to the type of the Duffing oscillator

Now let us increase the value of the additional nonlinearity parameter β . It should be noted that the nonlinear parameter β , from the point of view of oscillatory regimes in a separate oscillator, is responsible for the deviation of the shape of the potential “well” from the classical quadratic one. The resulting oscillations become non-isochronous, i.e. their period depends on the amplitude. From the point of view of synchronization, this factor leads to an increase in the synchronization area, the larger the parameter β , as indicated in Ref. [34]. Therefore, in the case of large values of this parameter, one can expect both stronger resonances and the destruction of quasi-periodic bifurcations due to them. We will discuss these effects in section 3.

Fig. 6 shows similar to Fig. 4 graphs of Lyapunov exponents depending on the magnitude of the coupling μ for $\beta = 2$ and 3. In the case of $\beta = 2$, Fig. 6, *a* shows a cascade of the Neimark-Sacker (NS) bifurcation of an invariant curve from equilibrium E and quasi-periodic Hopf bifurcations $QH_{1,2,3}$. There are practically no resonances in this area. A “thickening” sufficiently pronounced four-frequency resonances is observed on the right as we approach the higher frequency point QH_4 . However, the

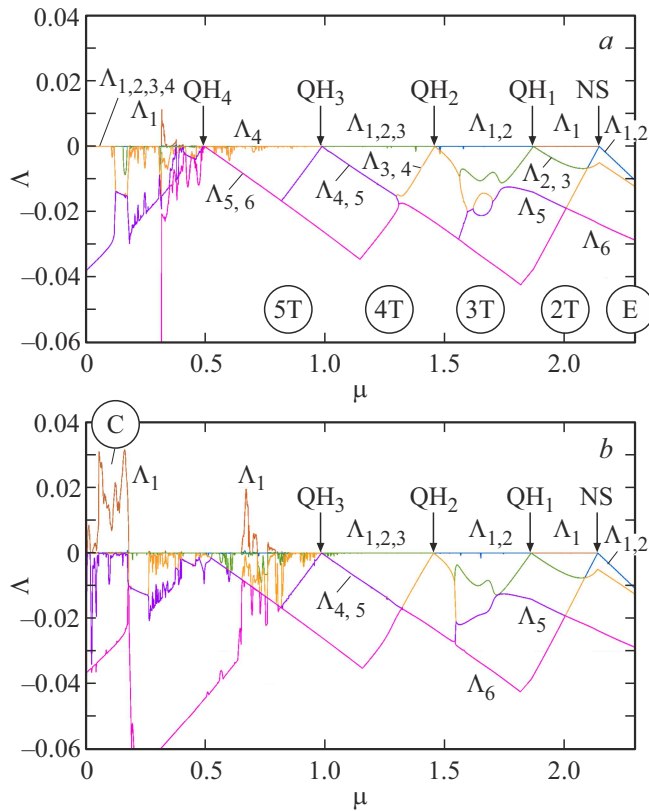


Figure 6. Graphs of Lyapunov exponents depending on the magnitude of the coupling μ for $\Delta = 30$: *a* — $\beta = 2$, *b* — $\beta = 3$. Values of the other parameters: $\lambda_1 = 0.5$, $\lambda_2 = 1$, $\lambda_3 = 1.5$, $\lambda_4 = 2$, $\lambda_5 = 2.5$, $\varepsilon = 0.1$.

characteristic condition for a quasi-periodic Hopf bifurcation $\Lambda_5 = \Lambda_6$ is preserved in its vicinity. At the same time, the six-frequency regime practically does not occur to the left of this point. There is an irregular alternation of windows of five- and four-frequency regimes, and even narrow areas of three-frequency regime and chaos with $\Lambda_1 > 0$ are possible.

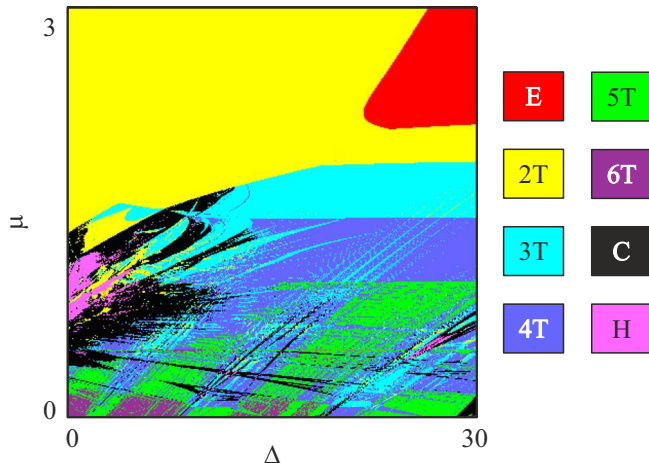


Figure 7. Chart of Lyapunov exponents for $\beta = 3$. The values of the other parameters are similar to Fig. 2.

A five-frequency regime with $\Lambda_{1,2,3,4} = 0$ is implemented when the coupling is further reduced, as it approaches the point $\mu = 0$.

Let's move on to the case of $\beta = 3$, Fig. 6, *b*. Now, only points NS and $QH_{1,2}$ are reliably observed. „Accumulation“ of small three-frequency resonances takes place on the right in the vicinity of point QH_3 , and accumulation of four-frequency resonances takes place on the left. An alternation of regime windows of different types is again observed with a further decrease coupling, mainly four-frequency and chaos, but excluding six-frequency ones. In contrast to the case of Fig. 6, *a*, all tori are destroyed with a small coupling μ — a fairly wide window of chaos *C* appears.

Fig. 7 shows the Lyapunov chart for the case $\beta = 3$. It should be compared with Fig. 2, *a*. Dynamics is observed along the right edge of the chart, corresponding to the graphs in Fig. 6, *b*. There are no resonances in the two-frequency 2T and three-frequency 3T regimes in the central part of the chart. There are tongues of three-frequency regimes in the four-frequency range of 4T. Pronounced tongues are not observed below, with a lower coupling μ , but a somewhat irregular alternation of regimes occurs. With frequency detunings $\Delta < 17.7$, six-frequency regimes are restored. It is interesting to trace the nature of the regimes at small Δ with an increase in the value of coupling μ . First, a six-frequency regime is implemented, which switches to a five-frequency or four-frequency regime. They then collapse to form chaos. At the same time, the areas of chaos noticeably increase compared to Fig. 2, *a*. Another feature is the appearance of hyperchaos *H*. With a sufficiently large coupling, quasi-periodic oscillations are restored immediately from chaos, and in the form of a two-frequency 2T regime. Thus, large values of additional nonlinearity of the Duffing oscillator type enhance resonances and contribute to the destruction of synchronization and the possible destruction of quasi-periodic bifurcations of invariant tori.

Conclusion

The effect of quasi-periodic resonances on the Landau-Hopf scenario can be studied using the example of an ensemble of discrete van der Pol oscillators, taking into account additional nonlinearity of the Duffing oscillator type. With small frequency detunings of the oscillators, tongues of quasi-periodic regimes arise, similar to Arnold's tongues, and in the region of the highest frequency oscillations. There is chaos in the area where such tongues overlap. With a large frequency detuning of the oscillators, the general structure of Landau-Hopf regime transformation remains, but the quasi-periodic Hopf bifurcation in the cascade can be replaced by a saddle-node torus bifurcation in the narrow vicinity of the bifurcation point. Narrow resonance regions based on tori of different dimensions are also observed, and secondary resonances may occur on resonant tori. There are virtually no resonances for low-dimensional tori. When the nonlinearity parameter is increased by the type of Duffing oscillator, resonances can destroy high-dimensional tori in the Landau-Hopf cascade. At the same time, there is an irregular alternation of torus windows of different dimensions and chaos. However, this requires a rather large amount of nonlinearity.

It should be noted that, due to the universality of the approaches of nonlinear oscillation theory, the results obtained may be of interest for various specific fields. Quasi-periodic oscillations are quite common in radio electronics, radiophysics, astrophysics, laser physics, climatology, etc. In this case, there may be situations when multi-frequency oscillations are observed, characterized by a set of incommensurable frequencies. However, such cases have been little studied. The influence of certain factors on such fluctuations and the „strength“ of possible resonances is of interest. The tools and approaches of the nonlinear theory of oscillations and the theory of dynamical systems are effective in this case. In this regard, the method of charts of Lyapunov exponents can serve as universal and informative.

Funding

This study has been carried out under the state assignment of the Kotel'nikov Institute of Radio Engineering and Electronics of the RAS (FFWZ-2025-0016).

Conflict of interest

The authors declare that they have no conflict of interest.

References

- [1] P.S. Lindsay, A.W. Cumming. *Physica D*, **40** (2), 196 (1989). DOI: 10.1016/0167-2789(89)90063-8
- [2] L. Borkowski, P. Perlikowski, T. Kapitaniak, A. Stefanski. *Phys. Rev. E*, **91** (6), 062906 (2015). DOI: 10.1103/PhysRevE.91.062906
- [3] I. Manimehan, K. Thamilmaran, P. Philominathan. *Int. J. Bifurcation Chaos*, **21** (7), 1987 (2011). DOI: 10.1142/S0218127411029586
- [4] V. Anishchenko, S. Nikolaev, J. Kurths. *Phys. Rev. E*, **73** (5), 056202 (2006). DOI: 10.1103/PhysRevE.73.056202
- [5] V.S. Anishchenko, S.M. Nikolaev. *Int. J. Bifurcation Chaos*, **18** (9), 2733 (2008). DOI: 10.1142/S0218127408021956
- [6] V.S. Anishchenko, S.M. Nikolaev. *Rus. J. Nonlin. Dyn.*, **2** (3), 267 (2006). DOI: 10.20537/nd0603001
- [7] N. Inaba, K. Kamiyama, T. Kousaka, T. Endo. *Physica D*, **311**, 17 (2015). DOI: 10.1016/j.physd.2015.08.008
- [8] A.P. Kuznetsov, S.P. Kuznetsov, N.A. Shchegoleva, N.V. Stankevich. *Physica D*, **398**, 1 (2019). DOI: 10.1016/j.physd.2019.05.014
- [9] A.P. Kuznetsov, Yu.V. Sedova, N.V. Stankevich. *Differentsial'nye uravneniya i processy upravleniya*, **1**, 54 (2023) (in Russian). DOI: 10.21638/11701/spbu35.2023.105
- [10] A.P. Kuznetsov, I.R. Sataev, Y.V. Sedova. *J. Appl. Nonlin. Dyn.*, **7** (1), 105 (2018). DOI: 10.5890/JAND.2018.03.009
- [11] N.G. Koudafoke, C.H. Miwadinou, A.V. Monwanou, A.L. Hinvi, J.C. Orou. *J. Dyn. Control*, **8** (3), 779 (2020). DOI: 10.1007/s40435-019-00595-w
- [12] A.E. Botha, Y.M. Shukrinov, J. Tekić, M.R. Kolahchi. *Phys. Rev. E*, **107** (2), 024205 (2023). DOI: 10.1103/PhysRevE.107.024205
- [13] T. Bakri, Y.A. Kuznetsov, F. Verhulst. *J. Dyn. Differ. Equat.*, **27**, 371 (2015). DOI: 10.1007/s10884-013-9339-9
- [14] A.N. Kulikov. *Differen. Equat.*, **48**, 1258 (2012). DOI: 10.1134/S0012266112090066
- [15] A.N. Kulikov, D.A. Kulikov. *Theor. Mathem. Phys.*, **203** (1), 501 (2020). DOI: 10.1134/S0040577920040066
- [16] N.M. Evstigneev. *Open J. Fluid Dyn.*, **6** (4), 496 (2016). DOI: 10.4236/ojfd.2016.64035
- [17] J. Sánchez Umbría, M. Net. *Phys. Fluids*, **33** (11), 114103 (2021). DOI: 10.1063/5.0064465
- [18] F. Garcia, J. Ogbonna, A. Giesecke, F. Stefani. *F. Commun. Nonlinear Sci. Numer. Simul.*, **118**, 107030 (2023). DOI: 10.1016/j.cnsns.2022.107030
- [19] R.A. Remillard, M.P. Muno, J.E. McClintock, J.A. Orosz. *Astrophys. J.*, **580** (2), 1030 (2002). DOI: 10.1086/343791
- [20] A.R. Ingram, S.E. Motta. *New Astronomy Rev.*, **85**, 101524 (2019). DOI: 10.1016/j.newar.2020.101524
- [21] M. Sekikawa, N. Inaba, K. Kamiyama, K. Aihara. *Chaos*, **24** (1), 013137 (2014). DOI: 10.1063/1.4869303
- [22] S. Hidaka, N. Inaba, M. Sekikawa, T. Endo. *Phys. Lett. A*, **379** (7), 664 (2015). DOI: 10.1016/j.physleta.2014.12.022
- [23] K. Kamiyama, N. Inaba, M. Sekikawa, T. Endo. *Physica D*, **289**, 12 (2014). DOI: 10.1016/j.physd.2014.09.001
- [24] A.P. Kuznetsov, Y.V. Sedova. *Int. J. Bifurcation Chaos*, **24** (7), 1430022 (2014). DOI: 10.1142/S0218127414300225
- [25] A.P. Kuznetsov, Y.V. Sedova, N.V. Stankevich. *Int. J. Bifurcation Chaos*, **33** (15), 2330037 (2023). DOI: 10.1142/S0218127423300379
- [26] L.D. Landau. *Dokl. Akad. Nauk USSR.*, **44**, 311 (1944).
- [27] E.A. Hopf. *Commun. Pure Appl. Mathem.*, **1** (4), 303 (1948).
- [28] A.N. Kulikov. *J. Mathem. Sci.*, **262** (6), 809 (2022). DOI: 10.1007/s10958-022-05859-z
- [29] R. Herrero, J. Farjas, F. Pi, G. Orriols. *Chaos*, **32** (2), 023116 (2022). DOI: 10.1063/5.0069878

[30] R. Herrero, J. Farjas, F. Pi, G. Orriols. *Multiplicity of Time Scales in Complex Systems: Challenges for Sciences and Communication II* (Springer Nature, Switzerland, 2023), p. 463. DOI: 10.1007/16618_2023_69

[31] D. Ruelle, F. Takens. *Les rencontres physiciens-mathématiciens de Strasbourg-RCP25* (1971), 12, p. 1.

[32] V.S. Afraimovich, L.P. Shilnikov. Amer. Math. Soc. Transl., **149** (2), 201 (1991). DOI: 10.1090/trans2/149/12

[33] A.P. Kuznetsov, S.P. Kuznetsov, I.R. Sataev, L.V. Turukina. Phys. Lett. A, **377** (45–48), 45 (2013). DOI: 10.1016/j.physleta.2013.10.013

[34] A. Pikovsky, M. Rosenblum, J. Kurths. *Synchronization. A universal concept in nonlinear sciences* (Cambridge university press, 2001), DOI: 10.1017/CBO9780511755743

[35] A.P. Kuznetsov, E. S. Seliverstova, D.I. Trubetskoy, L.V. Tyuryukina. Izvestiya vuzov. PND, **22** (4), 3 (2014) (in Russian). DOI: 10.18500/0869-6632-2014-22-4-3-42

[36] A.P. Kuznetsov, L.V. Turukina. Physica D, **470**, 134425 (2024). DOI: 10.1016/j.physd.2024.134425

[37] V.I. Arnold. Izvestiya AN SSSR. Ser. matematicheskaya, **25** (1), 21 (1961) (in Russian).

[38] V.I. Arnold. Chaos, **1** (1), 20 (1991). DOI: 10.1063/1.165812

[39] R. Vitolo, H. Broer, C. Simó. Regular Chaotic Dynamics, **16**, 154 (2011). DOI: 10.1134/S1560354711010060

[40] M. Komuro, K. Kamiyama, T. Endo, K. Aihara. Int. J. Bifurcation Chaos, **26** (7), 1630016 (2016). DOI: 10.1142/S0218127416300160

[41] R. Vitolo, H. Broer, C. Simó. Nonlinearity, **23** (8), 1919 (2010). DOI: 10.1088/0951-7715/23/8/007

[42] N.V. Stankevich, N.A. Shchegoleva, I.R. Sataev, A.P. Kuznetsov. J. Comput. Nonlin. Dyn., **15** (11), 111001 (2020). DOI: 10.1115/1.4048025

[43] N.C. Pati. Chaos, **34** (8), 083126 (2024). DOI: 10.1063/5.0208457

[44] A.G. Balanov, N.B. Janson, D.E. Postnov, O. Sosnovtseva. *Synchronization: from simple to complex* (Springer, Berlin, Heidelberg, 2009), DOI: 10.1007/978-3-540-72128-4

[45] A.P. Kuznetsov, J.P. Roman. Physica D, **238** (16), 1499 (2009). DOI: 10.1016/j.physd.2009.04.016

[46] A.P. Kuznetsov, J.P. Roman. Nonlinear Phenomena in Complex Systems, **12** (1), 54 (2009).

[47] G.M. Zaslavskii, R.Z. Sagdeev, D.A. Usikov, A.A. Chernikov. Soviet Phys. Usp., **31** (10), 887 (1988). DOI: 10.1070/PU1988v031n10ABEH005632

[48] G.M. Zaslavsky. *The physics of chaos in Hamiltonian systems* (Imperial College Press; Distributed by World Scientific, 2007), DOI: 10.1142/P507

[49] A.D. Morozov. *Rezonansy, cikly i haos v kvazikonservativnyh sistemah* (RHD, Moskva-Izhevsk, 2005) (in Russian).

Translated by A.Akhtyamov